

## Supplementary Information

### Phase stabilization via A-site ion anchoring for ultra-stable perovskite light emitting diodes

Shuo Ding <sup>a,b,c</sup>, Zhuoyuan Kong <sup>a,b,d</sup>, Piaoyang Shen <sup>a,b</sup>, Chunyan Wu <sup>a,b</sup>, Lei Qian <sup>a,b</sup>, Xinyu Zhang <sup>c</sup>, Hao Chen <sup>c\*</sup>, Chaoyu Xiang <sup>a,b\*</sup>

- a. *Laboratory of Optoelectronic Information Materials and Devices, Ningbo Institute of Materials Technology and Engineering, Chinese Academy of Sciences, Ningbo, Zhejiang, 315201, China*
- b. *Hangzhou Bay Laboratory of Advanced Nano–Optoelectronic Materials and Devices, Qianwan Institute of CNITECH, Ningbo, Zhejiang, 315300, China*
- c. *Department of Mechanical, Materials and Manufacturing Engineering, The University of Nottingham Ningbo China, Ningbo, Zhejiang, 315100, China*
- d. *Nano Science and Technology Institute, University of Science and Technology of China, Suzhou 215123, China*

\*Corresponding authors. Hao Chen (hao.chen@nottingham.edu.cn) and Chaoyu Xiang (xiangchaoyu@nimte.ac.cn).

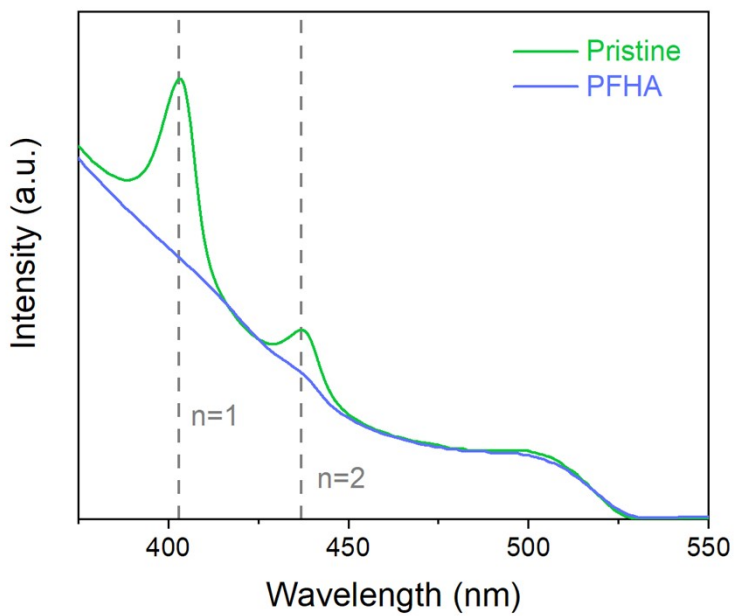


Fig. S1 | UV-Vis absorption spectra of pristine and PFHA perovskites.

Herein, n represents the number of layers alongside the thickness direction of the 2D phases.

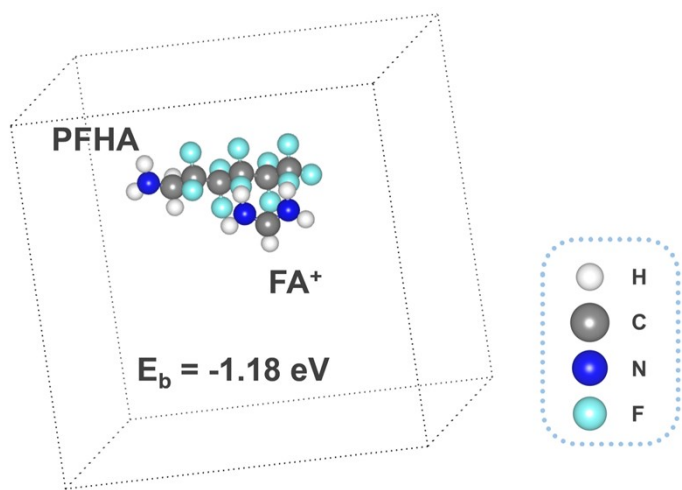


Fig. S2 | Representative configuration of PFHA coordination with FA<sup>+</sup>. The calculated binding energy is -1.18 eV.

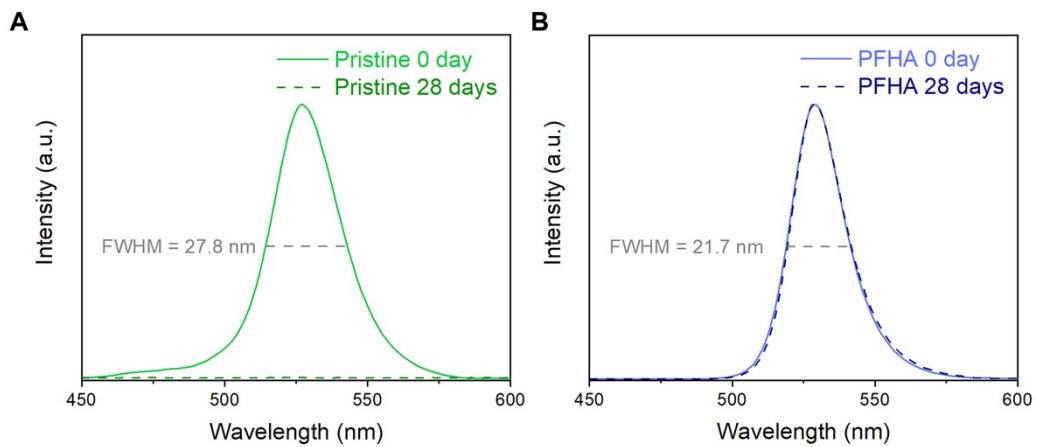


Fig. S3 | PL spectra of (A) pristine and (B) PFHA perovskite films upon 28 days ambient storage.

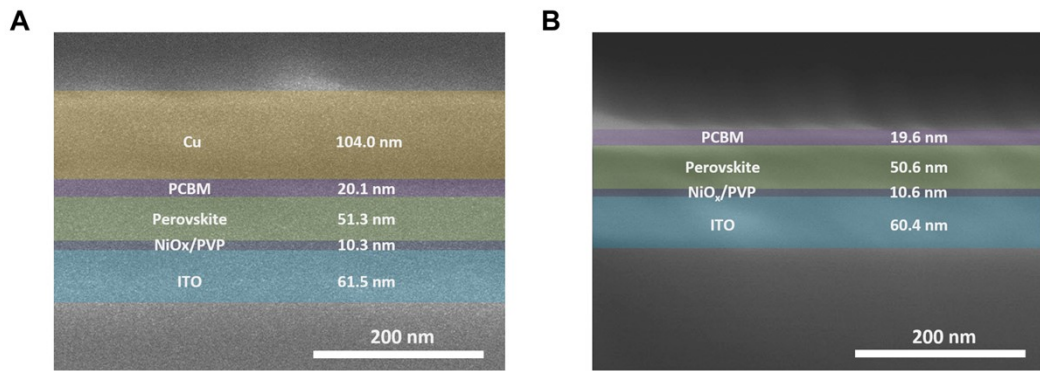


Fig. S4 | Cross-sectional SEM images for ion migration analysis. The device structure is ITO / NiO<sub>x</sub> / PVP / Perovskite / PCBM / Cu. (A) The entire device structure. (B) The device after the removal of the surface Cu electrodes using scotch tapes.

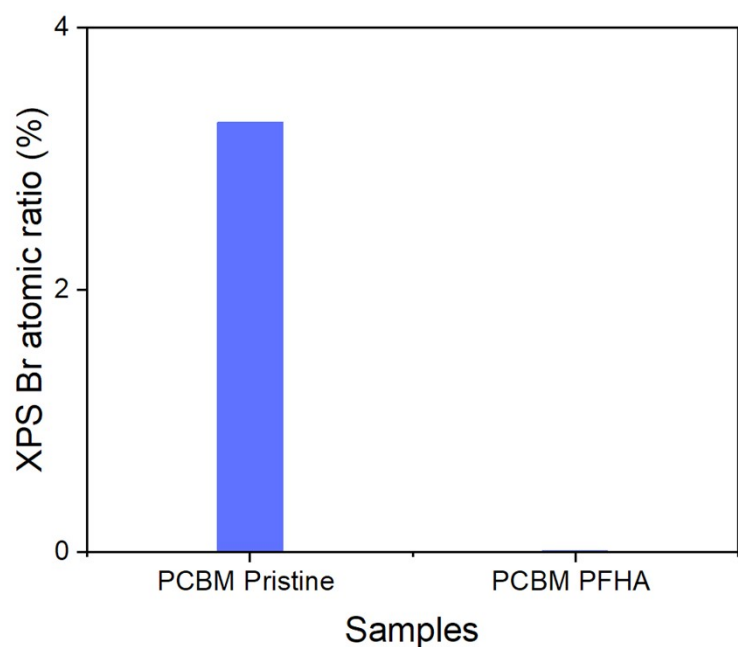


Fig. S5 | XPS Br atomic ratio of pristine and PFHA devices for ion migration analysis.

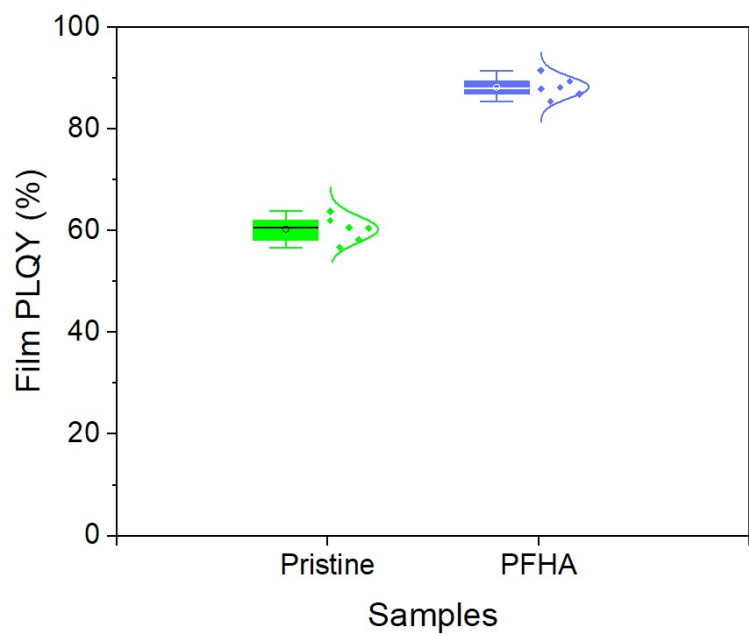


Fig. S6 | PLQY box plots for pristine and PFHA anchored perovskites. In the box plots, the middle bar represents the median, and the box represents the interquartile range; bars extend to  $1.5 \times$  the interquartile range.

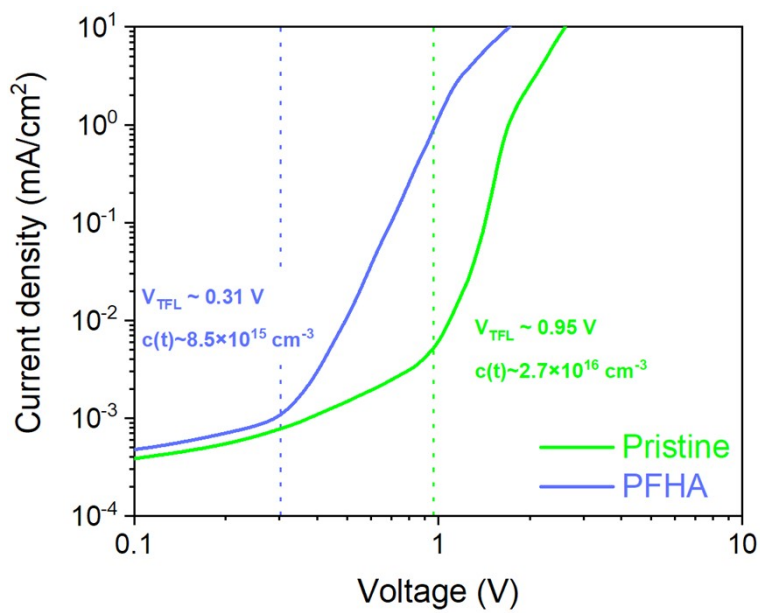


Fig. S7 | Current density versus voltage curve for hole-only devices. Device structure: indium tin oxide (ITO) / nickel oxide (NiOx) / polyvinyl pyrrolidone (PVP) / perovskite / molybdenum oxide (MoOx) / Au.

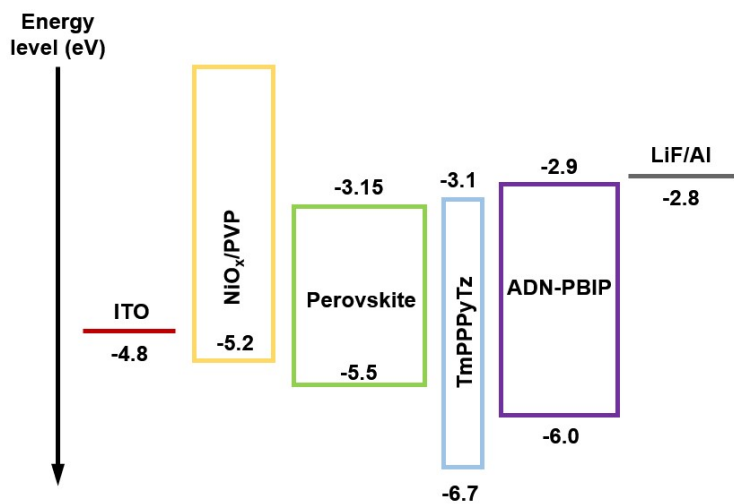


Fig. S8 | Device structure and corresponding energy levels of different layers in PeLEDs.

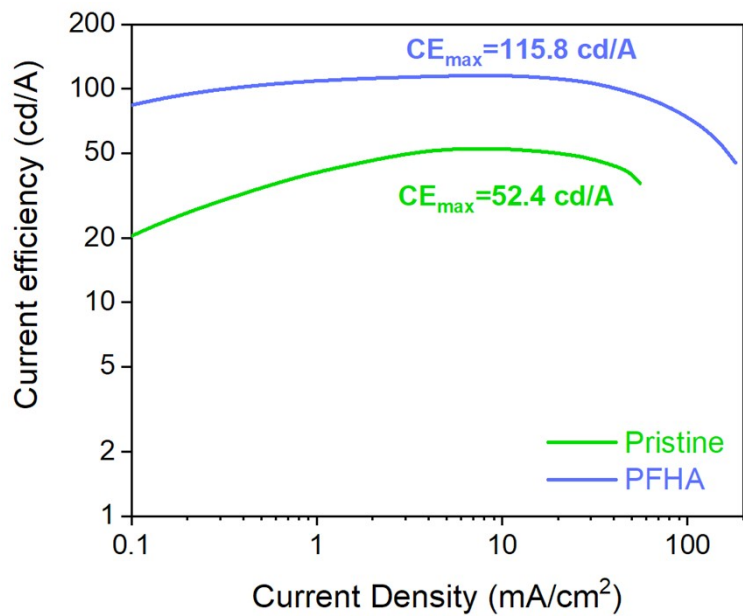


Fig. S9 | Current efficiencies (CE) versus current density of both PeLEDs.

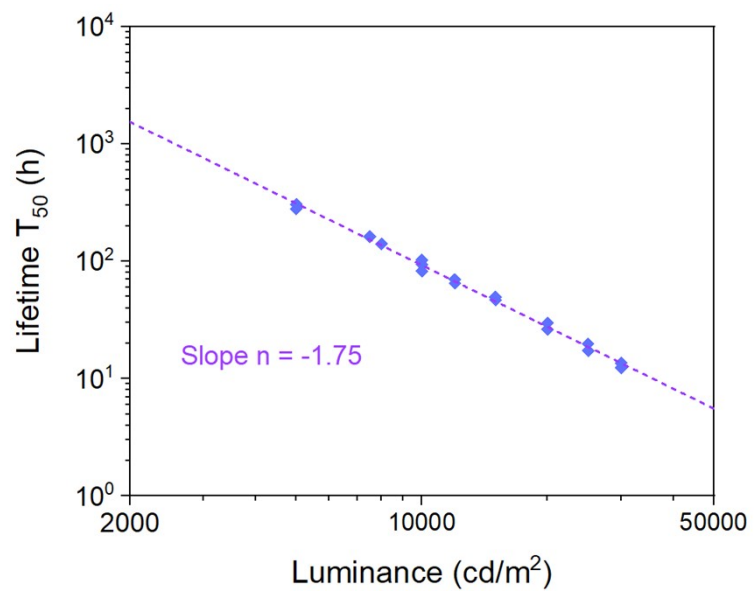


Fig. S10 | Equivalent operational lifetime  $T$  is calculated with the relationship of  $\frac{T}{T_0} = \left(\frac{L}{L_0}\right)^n$ . The calculated  $T_{50}$  lifetime at 100 cd/m<sup>2</sup> is over 326,252 hours with the slope  $n$  of -1.75.

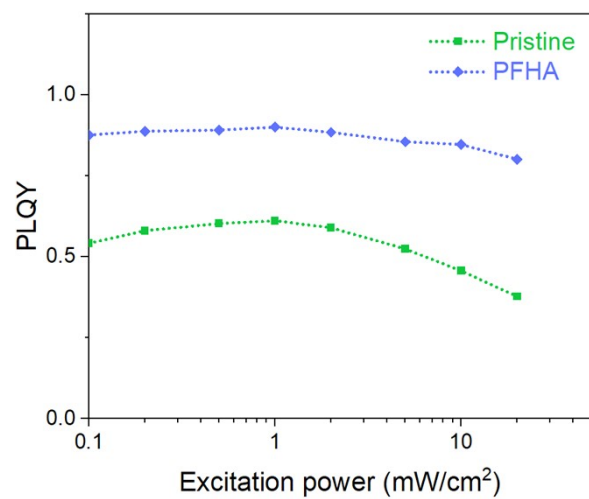


Fig. S11 | Excitation-dependent PLQY of pristine and PFHA films.

**Table S1 |** Performance of reported green perovskite LEDs with EQE exceeding 20% without optical outcoupling designs.

Perovskites	EQE <sub>max</sub> (%)	CE <sub>max</sub> (cd/A)	Operational lifetime (T <sub>50</sub> , min, reported)	Operational lifetime (T <sub>50</sub> , hour, equivalent at 100 cd/m <sup>2</sup> )	Ref.
FPEABr: CsPbBr <sub>3</sub> , quasi-2D	20.36	64	6.5 (L <sub>0</sub> =10,000 cd/m <sup>2</sup> )	342.6	<sup>1</sup>
BABr: CsPbBr <sub>3</sub> , quasi-2D	20.5	63	25 (L <sub>0</sub> =1000 cd/m <sup>2</sup> )	23.4	<sup>2</sup>
PEABr:(Cs, FA)PbBr <sub>3</sub> , quasi-2D	21.4	80	117 (L <sub>0</sub> =100 cd/m <sup>2</sup> )	1.95	<sup>3</sup>
PEABr:(CsPbBr <sub>3</sub> , quasi-2D	22.49	59.2	52 (L <sub>0</sub> =144 cd/m <sup>2</sup> )	1.6	<sup>4</sup>
PEABr: FAPbBr <sub>3</sub> , quasi-2D	22.9	98	390 (L <sub>0</sub> =100 cd/m <sup>2</sup> )	6.5	<sup>5</sup>
FA <sub>0.9</sub> GA <sub>0.1</sub> PbBr <sub>3</sub> , nanocrystals	23.4	108	132 (L <sub>0</sub> =100 cd/m <sup>2</sup> )	2.2	<sup>6</sup>
PEABr:(Cs, MA)PbBr <sub>3</sub> , quasi-2D	25.6	88	115 (L <sub>0</sub> =7,200 cd/m <sup>2</sup> )	3,411	<sup>7</sup>
PEABr: CsPbBr <sub>3</sub> , Quasi-core/shell nanoparticles	28.1	95.8	242.4 (L <sub>0</sub> =100 cd/m <sup>2</sup> )	4.0	<sup>8</sup>
((FA <sub>0.7</sub> MA <sub>0.1</sub> GA <sub>0.2</sub> ) <sub>0.87</sub> Cs <sub>0.13</sub> PbBr <sub>3</sub> ) core/shell	28.9	150.1	31,200 (L <sub>0</sub> =1,000 cd/m <sup>2</sup> )	29,241	<sup>9</sup>
PEABr: FAPbBr <sub>3</sub> , quasi-2D	29.5	124.0	1,120.2 (L <sub>0</sub> =12,000 cd/m <sup>2</sup> )	81,229	<sup>10</sup>
PEABr: FAPbBr <sub>3</sub> , quasi-2D	30.84	115.32	100.6 (L <sub>0</sub> =100.88 cd/m <sup>2</sup> )	1.7	<sup>11</sup>
PEABr: CsPbBr <sub>3</sub> , quasi-2D	32.1	111.7	213.6 (L <sub>0</sub> =100 cd/m <sup>2</sup> )	3.6	<sup>12</sup>
<b>FPEABr: FAPbBr<sub>3</sub>, quasi-2D</b>	<b>27.1</b>	<b>115.8</b>	<b>6,190 (L<sub>0</sub>=10,000 cd/m<sup>2</sup>)</b>	<b>326,252</b>	<b>This work</b>

EQE<sub>max</sub>, maximum external quantum efficiency; CE<sub>max</sub>, maximum current efficiency; L<sub>max</sub>, maximum luminance; T<sub>50</sub>, device operating half-life; L<sub>0</sub>, initial luminance. The equivalent T<sub>50</sub> lifetime at 100 cd/m<sup>2</sup> is calculated with the relationship of

$$T/T_0 = (L/L_0)^{-1.75}$$

## Reference

- 1 Y. Jiang, M. Cui, S. Li, C. Sun, Y. Huang, J. Wei, L. Zhang, M. Lv, C. Qin, Y. Liu and M. Yuan, *Nat. Commun.*, 2021, **12**, 336.
- 2 L. Kong, X. Zhang, Y. Li, H. Wang, Y. Jiang, S. Wang, M. You, C. Zhang, T. Zhang, S. V. Kershaw, W. Zheng, Y. Yang, Q. Lin, M. Yuan, A. L. Rogach and X. Yang, *Nat. Commun.*, 2021, **12**, 1246.
- 3 C. Sun, Y. Jiang, M. Cui, L. Qiao, J. Wei, Y. Huang, L. Zhang, T. He, S. Li, H.-Y. Hsu, C. Qin, R. Long and M. Yuan, *Nat. Commun.*, 2021, **12**, 2207.
- 4 Z. Chu, Q. Ye, Y. Zhao, F. Ma, Z. Yin, X. Zhang and J. You, *Adv. Mater.*, 2021, **33**, 2007169.
- 5 X. Peng, X. Yang, D. Liu, T. Zhang, Y. Yang, C. Qin, F. Wang, L. Chen and S. Li, *ACS Energy Lett.*, 2021, **6**, 4187–4194.
- 6 Y. H. Kim, S. Kim, A. Kakekhani, J. Park, J. Park, Y. H. Lee, H. Xu, S. Nagane, R. B. Wexler, D. H. Kim, S. H. Jo, L. Martínez-Sarti, P. Tan, A. Sadhanala, G. S. Park, Y. W. Kim, B. Hu, H. J. Bolink, S. Yoo, R. H. Friend, A. M. Rappe and T. W. Lee, *Nat. Photonics*, 2021, **15**, 148–155.
- 7 D. Ma, K. Lin, Y. Dong, H. Choubisa, A. H. Proppe, D. Wu, Y.-K. Wang, B. Chen, P. Li, J. Z. Fan, F. Yuan, A. Johnston, Y. Liu, Y. Kang, Z.-H. Lu, Z. Wei and E. H. Sargent, *Nature*, 2021, **599**, 594–598.
- 8 Z. Liu, W. Qiu, X. Peng, G. Sun, X. Liu, D. Liu, Z. Li, F. He, C. Shen, Q. Gu, F. Ma, H. Yip, L. Hou, Z. Qi and S. Su, *Adv. Mater.*, 2021, **33**, 2103268.
- 9 J. S. Kim, J.-M. Heo, G.-S. Park, S.-J. Woo, C. Cho, H. J. Yun, D.-H. Kim, J. Park, S.-C. Lee, S.-H. Park, E. Yoon, N. C. Greenham and T.-W. Lee, *Nature*, 2022, **611**, 688–694.
- 10 S. Ding, Q. Wang, W. Gu, Z. Tang, B. Zhang, C. Wu, X. Zhang, H. Chen, X. Zhang, R. Cao, T. Chen, L. Qian and C. Xiang, *Nat. Photonics*, 2024, **18**, 363–370.
- 11 W. Bai, T. Xuan, H. Zhao, H. Dong, X. Cheng, L. Wang and R. Xie, *Adv. Mater.*, 2023, **35**, 2302283.
- 12 S. Sun, J. Tai, W. He, Y. Yu, Z. Feng, Q. Sun, K. Tong, K. Shi, B. Liu, M. Zhu, G. Wei, J. Fan, Y. Xie, L. Liao and M. Fung, *Adv. Mater.*, DOI:10.1002/adma.202400421.